Intermodulation Crosstalk from Silicon Microring Modulators in Wavelength-Parallel Photonic Networks-on-Chip

Kishore Padmaraju[1], Noam Ophir[1], Aleksandr Biberman[1], Long Chen[2], Elizabeth Swan[3], Johnnie Chan[1], Michal Lipson[2], and Keren Bergman[1]

1: Department of Electrical Engineering, Columbia University, New York, New York, USA
2: School of Electrical and Computer Engineering, Cornell University, Ithaca, New York, USA
3: College of Optical Sciences, University of Arizona, Tucson, Arizona, USA
kpadmara@ee.columbia.edu

***Abstract* — We experimentally characterize the intermodulation crosstalk incurred by wavelength-parallel optical signals using a silicon microring resonator electro-optic modulator. We measure corresponding bit-error-rates and record eye diagrams, observing signal integrity degradation for varying wavelength channel spacing.**

Introduction

The continuing scalability trend associated with increasing the number of processing cores in chip multiprocessors has fostered the requirement for high-performance networks-on-chip, directing on-chip communication between processing cores, as well as off-chip communication for memory access. The resulting bandwidth requirements are quickly exceeding the capabilities of traditional electronics, generally limited by power dissipation, as well as electrical pin count and packaging constraints. Photonic networks-on-chip have the potential to alleviate the bandwidth bottleneck, and improve the overall power consumption. Here, silicon photonic components required for modulating, transmitting, routing, and receiving optical signals have all been individually demonstrated on a silicon-on-insulator (SOI) platform compatible with complementary metal-oxide-semiconductor (CMOS) [1–6].

The silicon microring resonator electro-optic modulator offers a small footprint (Fig. 1a), low power consumption, and high modulation rate. Using this device, error-free operation of up to 12.5-Gb/s modulation rates have been demonstrated [5]. Leveraging these devices in systems that maximize bandwidth using wavelength division multiplexing (WDM), multiple microring modulators can be cascaded along the same waveguide [6]. The wavelength selectivity of each modulator can be controlled by varying the radius of each microring during the fabrication process. Since each modulator in the cascade affects a single target wavelength channel, this alleviates the need for spectrally demultiplexing and multiplexing each wavelength channel for independent modulation. However, since the microring modulator encodes the optical data by shifting its resonance in and out of the target wavelength channel, neighboring wavelength channels will suffer from intermodulation crosstalk for sufficiently small wavelength channel spacing. A wavelength spectrum of the modulator presented in this work, in its passive and modulated states, is shown in Fig. 1b. When modulated, thermal dissipation from the electrical current yields a stable red shift of the resonance wavelength; carrier injection blue shifts the resonance wavelength, resulting in optical modulation. Because the wavelength spectrum is recorded for a much longer duration than the period of the modulation, the wavelength scan in Fig. 1b does not depict the instantaneous resonance of the microring; the spectrum represents an averaging over all the resonance states during modulation. The localization of the modulation indicates that neighboring channels higher in frequency to the modulated signal will be more adversely affected by intermodulation crosstalk.

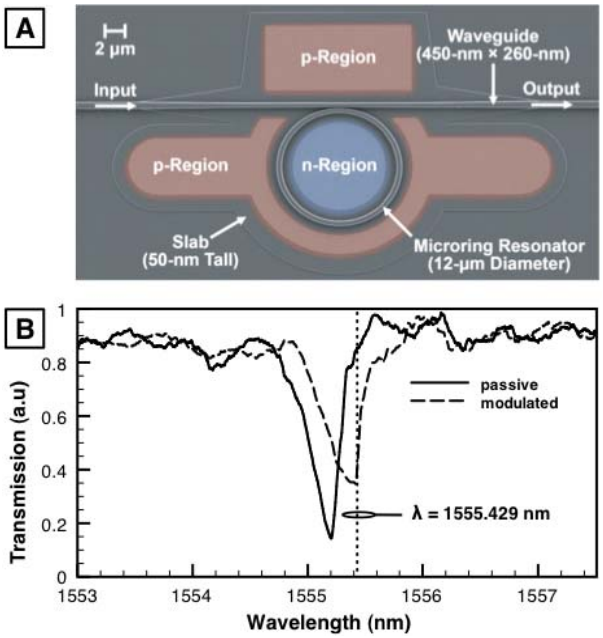

Fig. 1 a) Scanning-electron-microscope (SEM) image of the microring modulator. N and P doping are indicated in the interior and exterior of the microring, respectively. **b)**Wavelength spectrum of the micoring in its passive and modulated states. The wavelength of the modulated signal is indicated by a vertical dashed line.

Device and experimental setup

The device used in this experiment (Fig. 1a), fabricated at the Cornell Nanofabrication Facility, has a 6-μm microring resonator radius with waveguide dimensions of 450 nm × 260 nm. It was fabricated by patterning the SOI substrate using electron-beam lithography and reactive-ion etching, followed by doping using an ion implantation process.

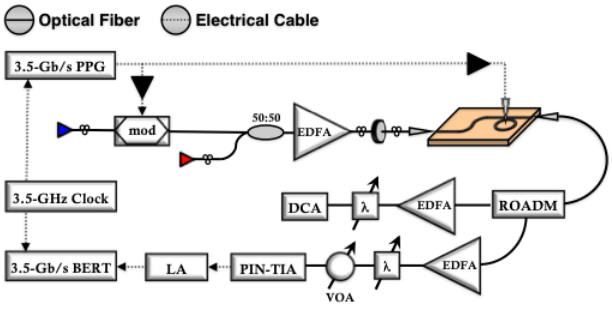

Fig. 2 Diagram of the experimental setup.

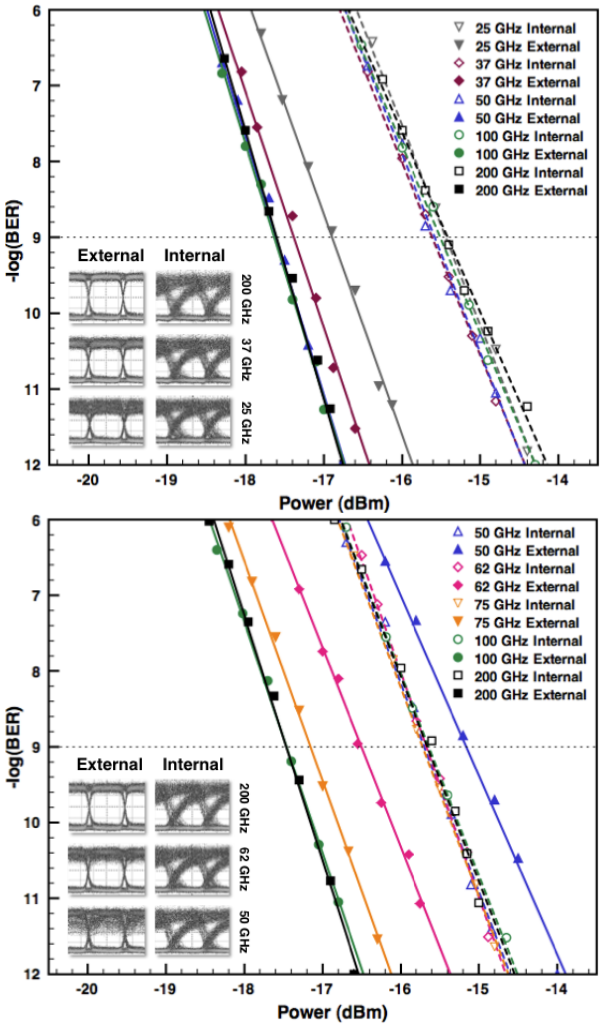

Fig. 3 Measured BERs when the external channel is frequency spaced below (**top**) and above (**bottom)** the internal channel. Eye diagrams at selected spacings (**insets**).

In our experimental setup (Fig. 2), we externally modulate a CW laser with a 3.5-Gb/s non-return to zero (NRZ) 2^7–1 pseudo-random bit sequence (PRBS) using a pattern generator and a commercial $LiNbO_3$ modulator. The externally modulated channel is passively combined with another CW laser at the wavelength of 1555.429 nm. This wavelength, corresponding to the resonance of the microring modulator, is kept constant throughout the duration of the experiment. The signals are amplified with an erbium-doped fiber amplifier (EDFA) before being launched into the chip using tapered fibers. Within the chip, the CW laser is internally modulated with a 3.5-Gb/s NRZ 2^7–1 PRBS using the microring modulator. The microring modulator is driven electrically with a 0.85-V voltage bias and a 2.1-V_{PP} electrical signal. The optical power of each wavelength channel is set to a combined 4 dBm of optical power launching into the chip, and have equal optical power coming off chip. Once off chip, the internally and externally modulated wavelength channels are filtered to the add and drop ports of a reconfigurable optical add-drop multiplexer (ROADM), respectively. Each wavelength channel undergoes amplification and filtering stages, before being received by either a digital communications analyzer (DCA) or

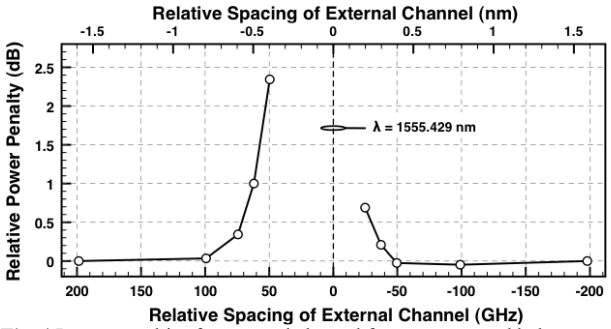

Fig. 4 Power penalties for external channel frequency spaced below (negative) and above (positive) the internal channel (set at zero).

a variable optical attenuator (VOA) followed by a PIN-TIA photodetector in conjunction with a limiting amplifier (LA). A BER tester (BERT) is used for BER measurements.

The externally modulated channel is initially spaced 200 GHz above the internally modulated channel. The spacing of the external channel is progressively reduced until it is 25 GHz above the internal channel, with eye diagrams and BER measurements being taken at every interval (Fig. 3). This procedure is repeated with the external channel initially spaced 200 GHz below the internal channel, with the spacing progressively increased until it is 50 GHz below the internal channel. Eye diagrams and BER measurements are also taken on the internally modulated channel at each interval (Fig. 3).

Results

The external channel is spaced as low as 50 GHz below the internal channel without incurring an additional power penalty relative to the 200-GHz spacing (Fig. 3). There is a 0.74-dB power penalty when the external channel is spaced 25 GHz below the internal channel. The external channel is spaced as low as 100 GHz above the internal channel without incurring additional power penalty (Fig. 3). At a spacing of 50 GHz above the internal channel, the external channel incurs a 2.47-dB power penalty. The power penalties show the expected asymmetry with respect to channel spacing (Fig. 4). The agreement between the BER measurements and eye diagrams of the internally modulated channel at every channel spacing indicates that the power penalty incurred by the externally modulated channel is from intermodulation crosstalk, and not due to the filtering stages following the chip.

Conclusion

We have shown that intermodulation crosstalk is a significant limiting factor for wavelength channel density in WDM systems utilizing cascaded silicon microring modulators.

We acknowledge support from the NSF and Semiconductor Research Corporation under grant ECCS-0903406 SRC Task 2001. The work of M. Lipson and L. Chen was part of the Interconnect Focus Center Research Program at Cornell University, supported in part by MARCO, Structured Materials Inc. under Grant 41594, and NSF CAREER Grant 0446571.

References

[1] S. Aseffa *et al.*, Nature **464**, 80 (2010).
[2] W. Bogaerts *et al.*, Optics Letters **32** (19), 2801, (2007).
[3] W. A. Zortman *et al.*, Proc. OFC 2010, OMI7 (2010).
[4] Q. Xu *et al.*, Optics Express **15** (2), 430 (2007).
[5] A. Biberman *et al.*, Optics Express **18** (15), 15544 (2006).
[6] B. G. Lee *et al.*, Photon. Technol. Lett, **19** (7), 456 (2007).